

Comment on “Global wave number-4 pattern in the southern subtropical sea surface temperature”

Elio Campitelli*

19 enero, 2021

Data: Hadley Centre SST (Rayner et al. 2003)

(Senapati, Dash, and Behera 2021) (SDB21 from now on) use Empirical Orthogonal Modes to detect a global wave-4 pattern in subtropical Sea Surface Temperatures (SST). However we have some doubts about the global nature of the phenomenon.

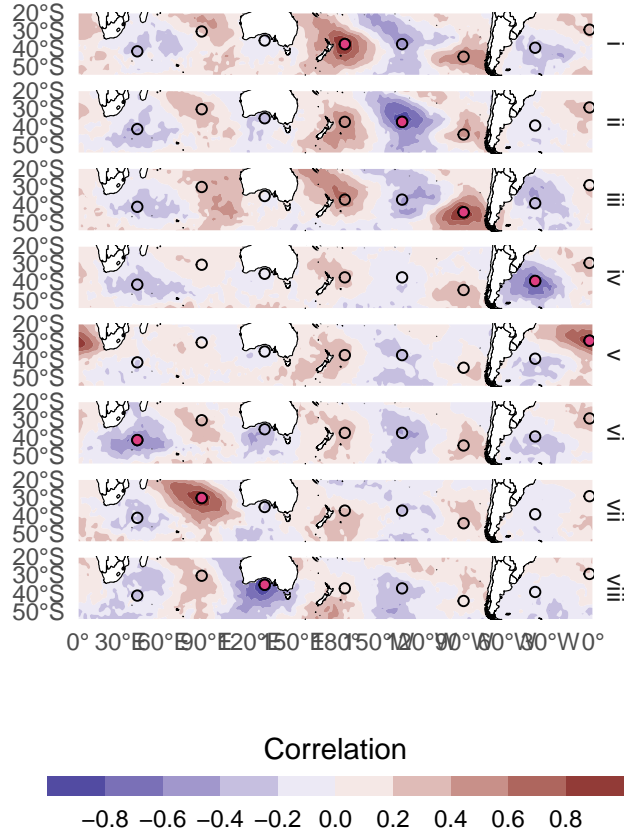


Figure 1: corelations

Figure 1 reproduces SDB21’s Figure 2 and show correlation maps of SST (with the leading EOF filtered out and with every other map with opposite sign) for the seven points of interest defined by SDB21, which are marked with dots. We believe that these maps are nowhere near as definitive in confirming the global nature of the wave-4 pattern. As pointed out by SDB21, SSTs South of Australia (point vii) shows virtually no relationship with any of the other points. But further than that, we see that the first tree points, located

*CIMA, elio.campitelli@cima.fcen.uba.ar

in the Pacific, are relatively well connected within each other but not nearly as much with the rest. This is further illustrated by Figure 2 which shows the explained variance of SST by the SST of each point. Points in the Pacific explain up to 40% of the variance of SST in some areas, while points in the other basins can barely explain 10% of the variance of the rest of global SST anomalies.

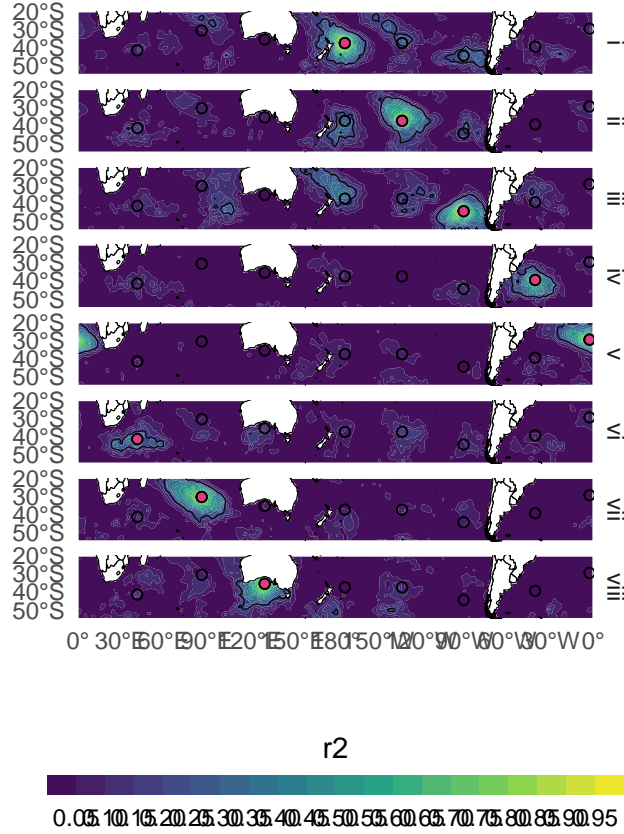


Figure 2: Coefficient of determination (r^2) computed from the correlations with the filtered SST in Figure 1. Contours only show areas with $r^2 > 0.1$. Black contour marks the 20% level, which is the median r^2 of the minimum correlation in correlation maps computed using 500 random points.

To better quantify how significant are the levels of connectivity shown in Figure 2, we computed the r^2 corresponding to the minimum correlation on correlation maps of 500 random points. The median explained variance 20% and 95% of random points had a coefficient of determination greater than 44%. With this in mind, values of the order of 20% in Figure 2 are on the order of what would be expected by chance.

Figures 1 and 2 do show that there are some relationships between regions and that the pattern of that relationship has a wave-4 structure. We are not saying that these relationships don't necessarily exist, but that they are not indicative of a globally coherent wave-4 oscillation. Rather, they are more indicative of separate but not independent phenomena.

This distinction further motivates us in splitting the wave-4 pattern into the Pacific basin (between 155°E and 290°E) and the Atlantic-Indian basins (the rest of the hemisphere). Then, we project each pattern onto the corresponding SST fields to get two indices. If the patterns are really coherent in time, then both indices must be strongly correlated. Figure 3 shows the relationship between the two indices (scales by their respective standard deviations). Again, while they are certainly not independent their correlation is only modest.

Figure 4 shows the correlation maps of SST with each index. Correlation values outside the area used to define each index (marked with gray overlay), although with a similar pattern, are relatively low.

We extend this analysis to all longitude sections of 90° of width (one wavelength). That is, for each longitude,

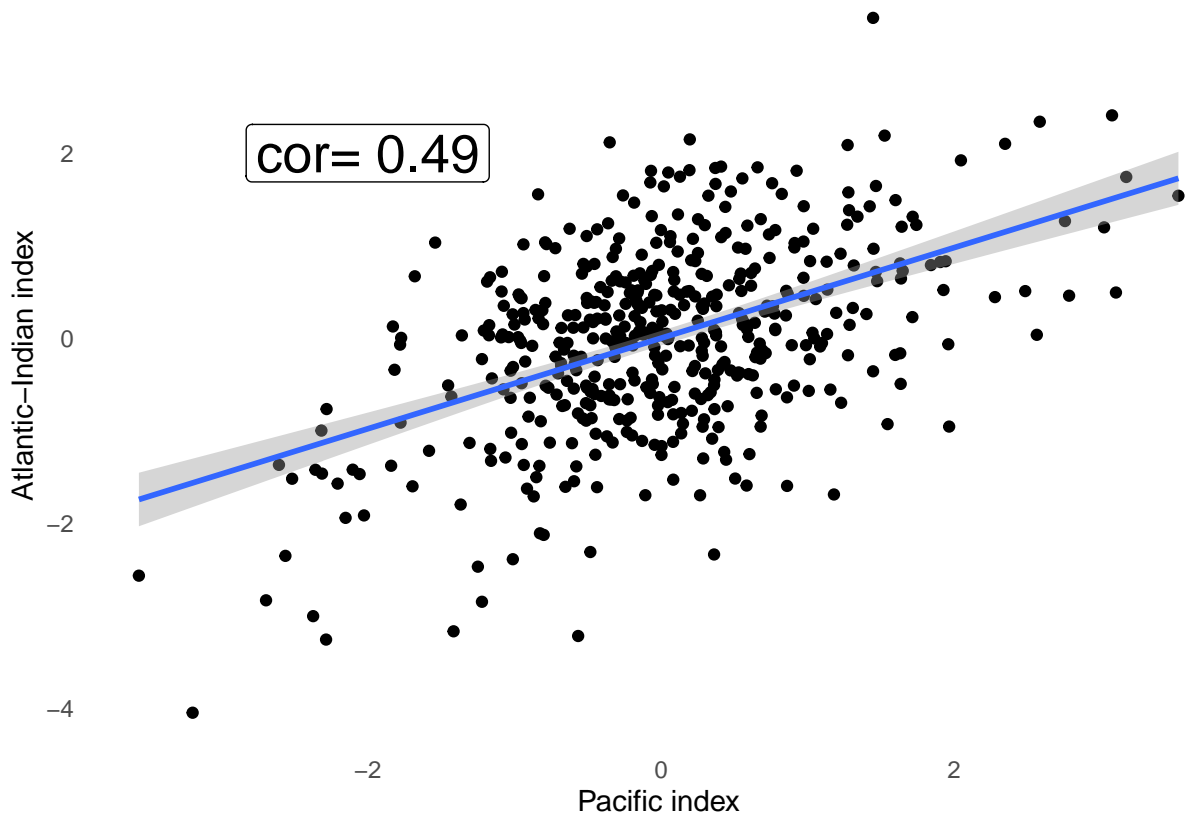


Figure 3: Relationship between the Pacific index and Atlantic-Indian index.

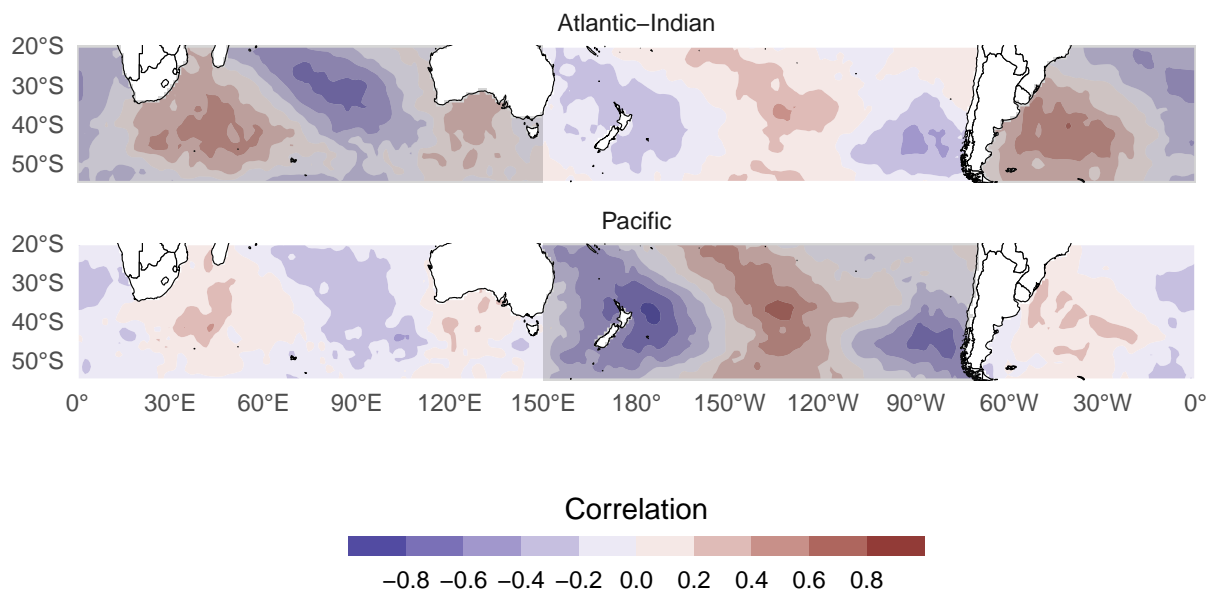


Figure 4: Correlation patterns with the Pacific index, the Atlantic-Indian index and the PC2.

take a 90° wide section of SST centred in that longitude and project the corresponding wave-4 pattern onto it to get a time-varying index. The result, then, is one “local wave-4 index” for each longitude.

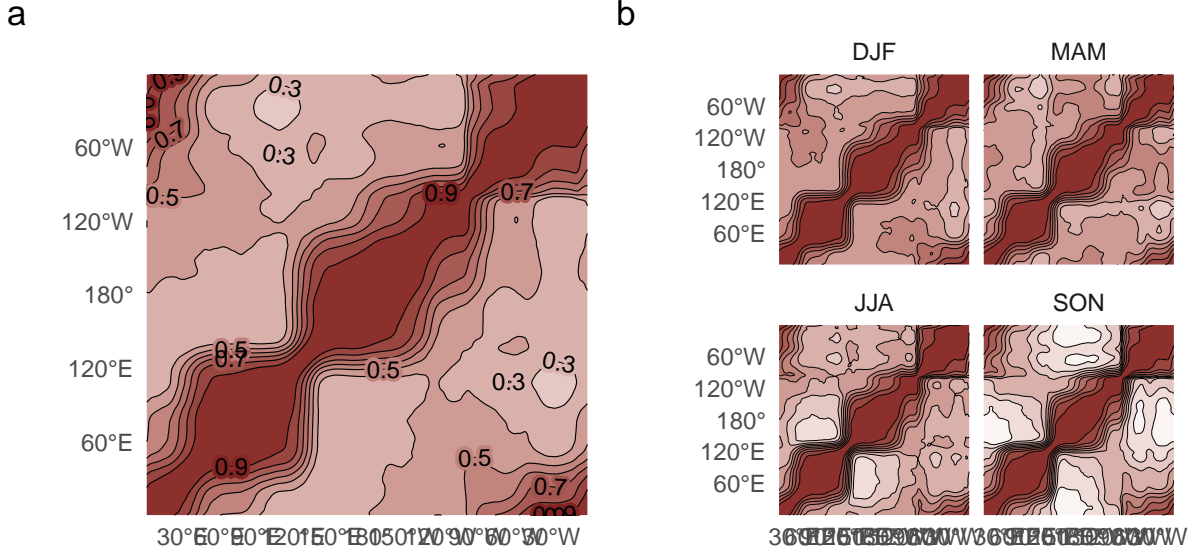
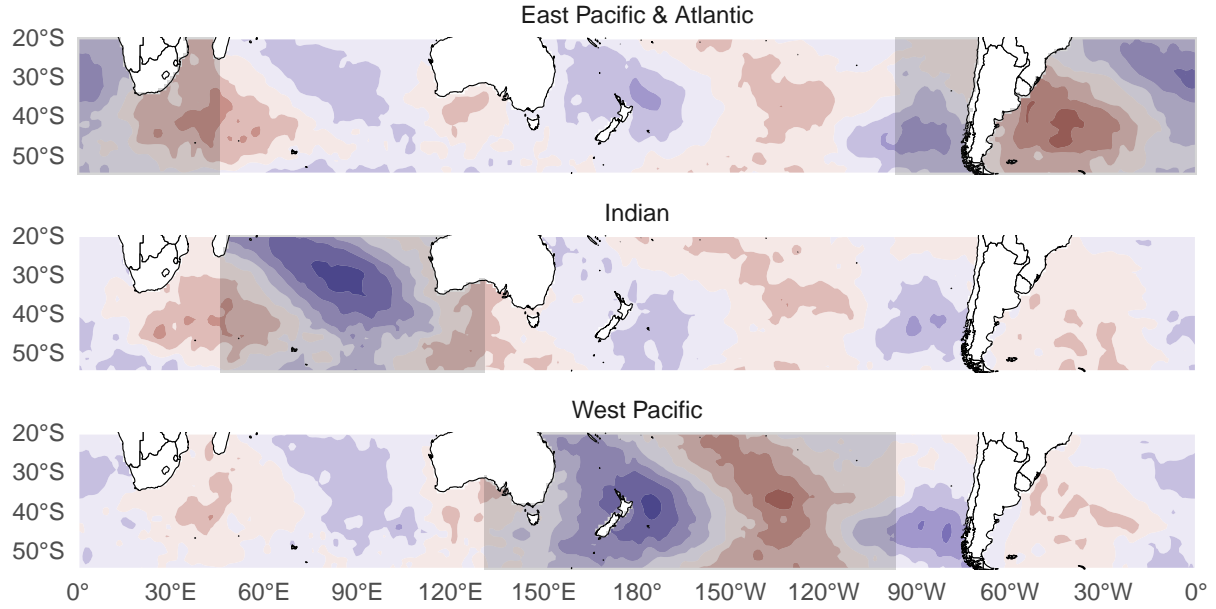


Figure 5: Pairwise correlation of “local wave-4” indices.

Figure 5a shows the pairwise correlation between all indices. There are three well-delineated longitude bands (approximately 45°E to 130°E , 95°W to 95°W and the rest of the domain) with high within-group correlations and low between group correlations. Perhaps not coincidentally, these correspond approximately to the three oceanic basins. Figure 5b shows pairwise correlations between indices by separated by trimester. Between-group correlations in Summer and Autumn are similar to the annual mean, but they are particularly low in Winter and Spring.

Based on these correlations, we use hierarchical clustering with $1 - \text{abs}(\text{correlation})$ as distance measure to classify each longitude into each of 3 groups. The clusters are flanked by the longitudes 46.5°E , 131.5°E , and 96.5°W , which agree well with the visual interpretation of Figure 5a. Using this classification, we now create three indices by again projecting the corresponding wave-4 pattern into SST anomalies.

(ref:patterns_k2-cap) Correlation maps between SST and each of the three basin-dependent wave-4 index. Overlayed in gray, the tree distinct areas of shared variability identified in Figure 5 by hierarchical clustering and selecting 3 clusters.



Correlation maps between SST anomalies and each of the three indices are shown in Figure @ref(fig:patterns_k). Inside the area used to define each index correlation are high and the pattern is well defined, as expected by construction. However, outside those areas, there is very little signal.

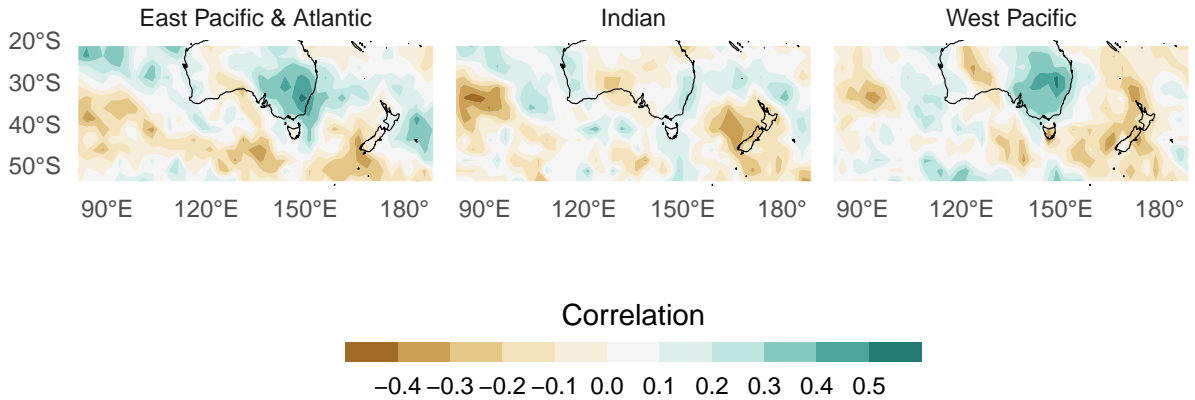


Figure 6: Correlation between each basin-wide wave-4 index and DJF-mean precipitation in New Zealand and neighbouring islands. Regions of p-values smaller than 0.05, adjusted by False Detection Rate within each map are shown in dots (there are no dots because there are no p-values smaller than 0.05).

Finally, we correlate each index with CPC Merged Analysis of Precipitation (Xie and Arkin 1997) in the region of New Zealand and neighbouring islands (Figure 6). The positive correlation in Southern Australia, found by SDB21 (their Figure 8), appears in relation to the East Pacific & Atlantic index and the West Pacific index (However, note that no correlation is statistically significant at the 95% level when p-values are adjusted for multiple comparisons (Benjamini and Hochberg 1995; Wilks 2016)), but not to the Indian part of the wave-4 pattern which is more evidence that the wave-4 pattern is not a coherent planet-wide pattern.

1 Acknowledgments

CMAF Precipitation data provided by the NOAA/OAR/ESRL PSL, Boulder, Colorado, USA, from their Web site at <https://psl.noaa.gov>

References

- Benjamini, Yoav, and Yosef Hochberg. 1995. “Controlling the False Discovery Rate: A Practical and Powerful Approach to Multiple Testing.” *Journal of the Royal Statistical Society: Series B (Methodological)* 57 (1): 289–300. <https://doi.org/10.1111/j.2517-6161.1995.tb02031.x>.
- Rayner, N. A., D. E. Parker, E. B. Horton, C. K. Folland, L. V. Alexander, D. P. Rowell, E. C. Kent, and A. Kaplan. 2003. “Global Analyses of Sea Surface Temperature, Sea Ice, and Night Marine Air Temperature Since the Late Nineteenth Century.” *Journal of Geophysical Research: Atmospheres* 108 (D14). <https://doi.org/10.1029/2002JD002670>.
- Senapati, Balaji, Mihir K. Dash, and Swadhin K. Behera. 2021. “Global Wave Number-4 Pattern in the Southern Subtropical Sea Surface Temperature.” *Scientific Reports* 11 (1): 142. <https://doi.org/10.1038/s41598-020-80492-x>.
- Wilks, D. S. 2016. “‘The Stippling Shows Statistically Significant Grid Points’: How Research Results Are Routinely Overstated and Overinterpreted, and What to Do About It.” *Bull. Amer. Meteor. Soc.* 97 (12): 2263–73. <https://doi.org/10.1175/BAMS-D-15-00267.1>.
- Xie, Pingping, and Phillip A. Arkin. 1997. “Global Precipitation: A 17-Year Monthly Analysis Based on Gauge Observations, Satellite Estimates, and Numerical Model Outputs.” *Bull. Amer. Meteor. Soc.* 78 (11): 2539–58. [https://doi.org/10.1175/1520-0477\(1997\)078%3C2539:GPAYMA%3E2.0.CO;2](https://doi.org/10.1175/1520-0477(1997)078%3C2539:GPAYMA%3E2.0.CO;2).